Distributed Mechanical Parameters Describing Vibration and Sound Radiation of Loudspeaker Drive Units

Wolfgang Klippel[1], Joachim Schlechter[2]

[1]University of Technology Dresden, Dresden, Germany, wklippel@klippel.de

[2]KLIPPEL GmbH, Dresden, Germany, schlechter@klippel.de

ABSTRACT

The mechanical vibration of loudspeaker drive units is described by a set of linear transfer functions and geometrical data which are measured at selected points on the surface of the radiator (cone, dome, diaphragm, piston, panel) by using a scanning technique. These distributed parameters supplement the lumped parameters (T/S, nonlinear, thermal), simplify the communication between cone, driver and loudspeaker system design and open new ways for loudspeaker diagnostics. The distributed vibration can be summarized to a new quantity called *accumulated acceleration level* (AAL) which is comparable with the sound pressure level (SPL) if no acoustical cancellation occurs. This and other derived parameters are the basis for modal analysis and novel decomposition techniques which make the relationship between mechanical vibration and sound pressure output more transparent. Practical problems and indications for practical improvements are discussed for various example drivers. Finally, the usage of the distributed parameters within finite and boundary element analyses is addressed and conclusions for the loudspeaker design process are made.

1. INTRODUCTION

Loudspeaker drive units (woofer, tweeter, micro-speakers, headphones) can be characterized by characteristics which are almost independent of the properties of the input signal. Such characteristics are resonance frequency, loss factor and other linear T/S parameters corresponding with an electrical equivalent circuit using lumped parameters. Nonlinear and thermal parameters have been introduced to assess the behavior of the loudspeaker in the large signal domain. Some of these parameters are single-valued numbers others are functions such as the electrical input impedance $Z(f)=U(f)/I(f)$ which is a function of frequency and the nonlinear parameter curves such as the stiffness $K_{ms}(x)$ versus displacement x. Those parameters of a particular drive unit describe with sufficient accuracy the relationship between voltage $u(t)$ and current $i(t)$ at the terminals and the driving force F_{coil} and the velocity V_{coil} of the voice coil as illustrated in Fig 1.

Unfortunately, the lumped parameters are bounded to the one-dimensional signal path and can not describe the multi-dimensional signal path via the mechanical system into the sound field. For describing the state of the radiator which could be a cone, dome, diaphragm, plate or panel we need a distributed model. Finite Element Analysis (FEA) may give valuable insight into the mechanical vibrations and is a powerful tool for designing cones and drive units. However, FEA requires detailed input information about the geometry and material parameters and is less suitable for the loudspeaker system design. System design needs characteristics which describe the acoustical output such as the sound pressure $p(\vec{r}_a)$ at a point $\vec{r}_a$ in the sound field. Acoustical measurements of the drive unit in free air without any enclosure are limited to low frequencies and have to be performed in the near field close to the

radiator. Measurements of the sound pressure in the far field require that the drive unit is mounted into a baffle, test box or other defined acoustical condition. Those standard measurements allow comparisons between different drive units but are not sufficient for optimizing the shape of the enclosure, horn and their interaction with the drive unit. Those tasks can be accomplished by acoustical FEA or boundary element analysis (BEA) which require the vibration and geometry of the radiator as input parameter.

This paper addresses the idea of using mechanical and geometrical characteristics of the radiator to describe loudspeaker drive units more comprehensively and to simplify the communication between driver and loudspeaker system design. In the first part of the paper basic parameters will be defined and general requirements on measurement and representation will be discussed. In the second part derived parameters will be presented which simplify the interpretation of the results. In the third part those new tools will be applied to example drive units to show new ways of loudspeaker diagnostics. Finally consequences to cone and system design are discussed.

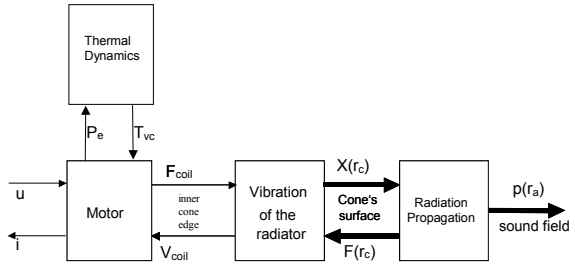

Fig 1: Modeling Loudspeaker drive units by a signal flow chart

2. PRIMARY VIBRATION PARAMETERS

The new parameters shall represent the mechanical and geometrical properties of the radiator which are important for the acoustical output. The calculation of the sound pressure requires the velocity $v_n(\vec{r_c})$ in normal direction on the radiator's surface and the precise position of this point $\vec{r_c}$. This information is taken from the whole surface of the radiator with sufficient spatial resolution giving a data set of distributed parameters.

However, most of the available scanning techniques measure the vibration rectangular to the scanned plane which is only identical to the surface for a flat radiator (panel).

The mechanical vibration of the radiator may also be affected by the acoustical load injecting a force $F(\vec{r_c})$ into the mechanical structure at point $\vec{r_c}$. This force is not negligible in headphones, microphones, micro-speakers, tweeters and other transducers where the mass of the radiator is relatively small.

2.1. Vibration Data

The characteristic describing the vibration of a radiator shall be independent of the particular excitation signal used during the measurement. Performing the measurement at sufficiently small amplitudes the loudspeaker may be considered as a linear system with a linear transfer function between a reference signal and the mechanical state signal at a point $\vec{r_c}$ on the radiator. The input voltage u at the terminals is a convenient reference signal but also the movement of the coil (e.g. velocity V_{coil}) may be used.

The displacement $X(\vec{r_c})$ of the radiator rectangular to the radiator's plane is easily accessible by sensors and available scanning techniques. The displacement can not only contain an a.c. signal but also a d.c. value generated by nonlinearities in the motor or suspension. Velocity, acceleration can be calculated from displacement by differentiation.

2.2. Transfer Function

The scanning process provides for each measurement point at position $\vec{r_c}$ on the radiator's surface a complex transfer function

$$H_x(j\omega,\vec{r_c}) = \frac{X(j\omega,\vec{r_c})}{U(j\omega)} \qquad (1)$$

where $X(j\omega,\vec{r_c})$ is the displacement rectangular to the radiator's plane and $U(j\omega)$ is the voltage at the loudspeaker terminals.

2.2.1. Amplitude and Phase Response

The complex transfer function $H_x(j\omega,\vec{r_c})$ can be described by the amplitude

$$L_{HX}(\omega,\vec{r_c}) = 20\log\left(\left|H_x(j\omega,\vec{r_c})\right|\frac{V}{mm}\right) \quad dB \qquad (2)$$

and the phase

$$\psi_{HX}(\omega,\vec{r_c}) = \arg(H_x(j\omega,\vec{r_c})) \quad (3)$$

2.3. Geometrical data

The position of each point $\vec{r_c}$ describes the shape of the surface of the scanned radiator and may be expressed in Cartesian coordinates

$$\vec{r_c} = x_c\vec{e_x} + y_c x\vec{e_y} + z_c\vec{e_z} \quad (4)$$

where y_c and z_c are in the scanned plane and x_c is the height rectangular to it.

Alternatively, the point may be defined in cylinder coordinates

$$\vec{r_c} = x_c\vec{e_x} + r\sin(\varphi)\vec{e_y} + r\cos(\varphi)\vec{e_z} \quad (5)$$

using radius r and angle φ.

3. SCANNING TECHNIQUE

3.1. Ambient Condition

The loudspeaker drive unit is measured in free air to consider the acoustical radiation load and viscous air flow. The test should be made at normal ambient temperature 15 C to 35 C, preferably at 20°C, relative humidity 25% to 75%, air pressure 86kPa to 106kPa as specified in IEC 60268-1.

Prior to the measurement the drive unit under test should be stored under those climate conditions for 24 hours.

Alternatively, the drive unit can be measured in vacuum to consider the mechanical components only.

3.2. Mounting Condition

The drive unit may be clamped in vertical or horizontal position and may be operated in free air, in a baffle or in the final loudspeaker enclosure. Since gravity may shift the voice coil position and change the stiffness of the suspension parts the mounting condition shall be stated.

3.3. Sensor

A non-contact measurement is mandatory to avoid a change of the mechanical impedance. For this reason an optical principle (laser technique) or an electrical principle (capacity sensor) are superior to accelerometer measurements. The size of the sensor should be small enough or the measurement distance should be large enough to keep the influence on the acoustical load minimal. Laser sensors based on the Doppler and triangulation principle measure the vibration at a good signal to noise ratio up to the frequency limit where the drive unit is used. While the Doppler laser gives primarily velocity the triangulation laser measures the distance between target and sensor and provides not only the vibration but also the geometry of the radiator at high precision.

3.4. Surface Coating

Some laser sensors require a special treatment of the radiator's surface with a white paint or power to generate a diffuse reflection. This reduces optical errors and increases the signal-to-noise ratio of the measured signal. In any case the layer of additional material should be thin enough to keep the effect on the vibration behavior negligible.

3.5. Excitation of the Loudspeaker

For the measurement of the linear transfer functions any stimulus with sufficient bandwidth may be used. It is recommend to shape the spectrum of the excitation signal to get the best signal-to-noise ratio at the sensor's output. A continuous sinusoidal sweep (chirp signal) may be used to separate the fundamental response from harmonic distortion.

3.6. Signal Processing

If the loudspeaker is excited by a repetitive signal the measured signals may be averaged to improve the signal-to-noise ratio. Afterwards the time signals are transferred into the frequency domain and the amplitude and phase of the transfer function is measured.

3.7. Measurement Grid

The scanning process performs a series of measurements on a two-dimensional grid on the radiator's surface. A grid in Cartesian or polar coordinates, according to Eq. *(4)* and *(5)* is recommended because those coordinates match the axial-symmetrical or rectangular geometry of most loudspeaker drive units and can easily be exported to FEA and BEA software.

3.8. Resolution

The resolution of the scan depends on the coordinate system and the number and distance of the measurement points. In a grid with constant angular resolution in polar coordinates the distance between the points in angular direction decreases with radius. Therefore there is a higher effective resolution near the center of the grid compared to a Cartesian grid. This is convenient for measuring the vibration on axial-symmetrical drivers as the dust cap still vibrates at higher frequencies and thus requires a higher grid resolution than the surround. For the same reason a polar grid may be also beneficial on rectangular panels when the origin of the grid is located at the center of the exciter. The surround of a circular drive unit may be scanned by a higher radial resolution than the cone to study the deformation of the surround geometry. 40 points in radial direction times 80 angular segments give a detailed scan which can reveal also irregularities in the vibration pattern that are limited to a small area.

However, scanning at high resolution is time consuming and produces a large amount of data which is not convenient for further mechanical and acoustical analyses using finite element and boundary element techniques. For axial-symmetrical drive units the angular resolution can be significantly reduced. Performing the scan at only one angle (dashed line in *Fig 2* gives already a rough approximation of the sound pressure response. Those differences are usually caused by circumferential modes which need a higher angular resolution. Using 16 angular subdivisions the SPL curve agrees almost perfectly with the one based on a high resolution scan.

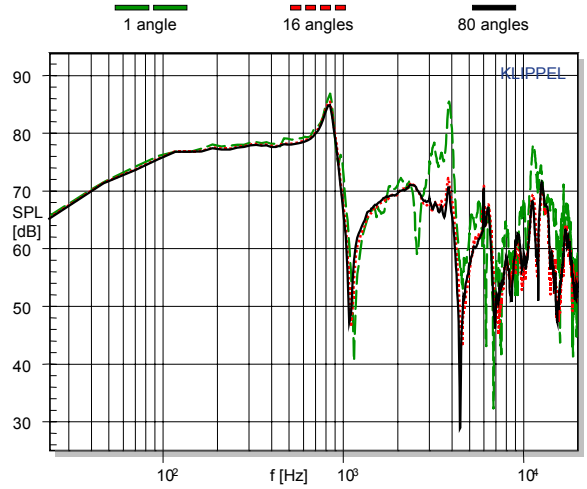

Fig 2: SPL response of woofer C calculated from a scanning using grids with 20 radii and different angular resolution: 1 angle (dashed line), 16 angles (dotted line) and 80 angles (solid lines).

The number of points in radial direction can also be significantly reduced while preserving the details of the SPL response. *Fig 3* shows for example the SPL response (dashed line) calculated by a scan using 5 equidistant radii which is an acceptable approximation at lower and medium frequencies where the woofer C with 12 cm diameter is used. Doubling the number of equidistant radii to 10 the SPL curve agrees almost perfectly with the result of the high resolution scan.

Thus, 100 – 200 points (about 16 angles and 10 radii) are usually sufficient for predicting the SPL response of an axial-symmetrical drive unit at high precision.

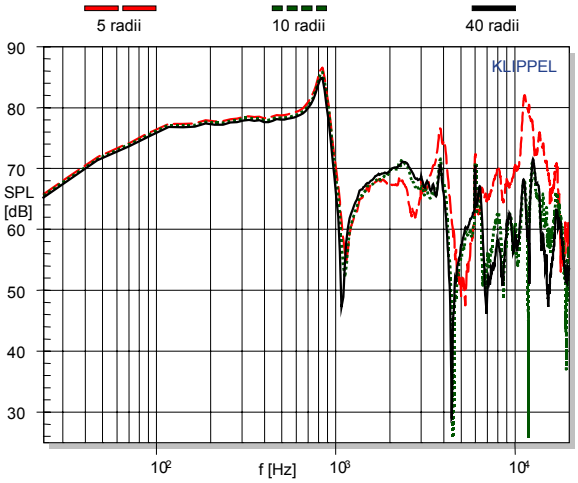

Fig 3: SPL response of woofer C calculated from a scanning using grids with 20 angles and different radial resolution: 5 radii (dotted line), 10 radii (dashed line) and 40 radii (solid line).

3.9. Optical Error Detection

A transparent or highly reflective surface, sharp edges or roughness of the structure may cause an optical problem, which may produce spikes, drop outs and other transients in the sensor output signal. Checking the signal-to-noise ratio is usually not sufficient to identify a corrupted measurement because those transients may contribute power to all frequencies. Most of the transient errors are reproducible if the measurement is repeated under identical conditions. Therefore, optical errors can only be detected if the position of the laser sensor is changed. This can easily be accomplished by changing the distance of the triangulation laser because the laser beam will hit the

target at almost the same spot but the sensor detects the reflected light at a slightly different angle and the errors appear differently in the measured signal. Then a correlation coefficient of the two signals can be calculated and a low correlation value indicates a measurement of low reproducibility due to an optical problem.

4. GRAPHICAL DISPLAY OF THE PARAMETERS

4.1. Frequency response

The amplitude and phase of the complex transfer function $H_x(j\omega,\vec{r}_c)$ can be displayed as a frequency response. This representation is useful for viewing a single point or comparing only few points. Of particular interest is the point r_{coil} where the driving force excites the radiator which is identical with the movement of the voice coil.

Fig 4 shows the amplitude response of the coil as solid line. Assuming that the driving force is almost constant the amplitude response here corresponds to the mechanical admittance of the radiator seen by the motor. This graphical display is useful for searching for the characteristic dip at the ring anti-resonance frequency f_{ra}=800 Hz which does not appear in the amplitude response of the surround shown as dashed line.

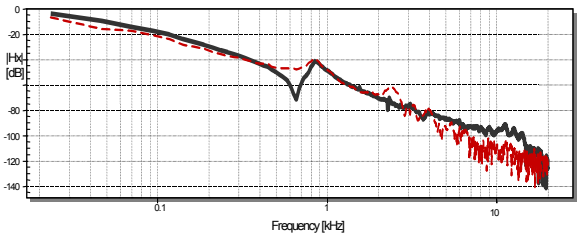

Fig 4: Magnitude response of the transfer function Hx(f)=X(f)/U(f) between voltage U and displacement X measured at the voice coil position (thick solid line) and at the surround (dashed line) of woofer C.

4.2. Geometry plots

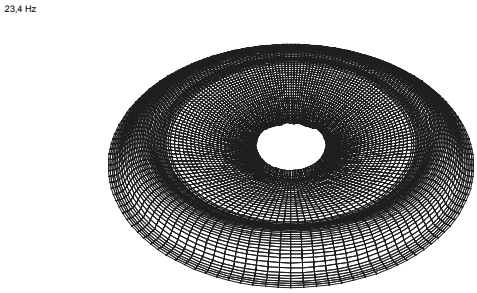

Fig 5: Geometry of the scanned cone surface of woofer A shown as a 3D wireframe

The geometry of the scanned surface may be displayed as a 2D cross section view or as a 3D wireframe as illustrated for woofer A in *Fig 5* where the grid nodes correspond to the measurement points.

4.3. Animations

To compare more easily the transfer function $H_x(j\omega,\vec{r}_c)$ of all scanned points on the radiator animation techniques have been developed which enhance important information in 2D and 3D displays. The amplitude of the vibration can be represented as color intensity while the instantaneous phase is coded by different colors as shown in *Fig 6*. The intensity plot reveals directly the nodes and antinodes.

A closer link between vibration and geometry can be produced by overlaying the displacement with the cross sectional view as shown in the upper part of *Fig 6* and with the complete 3D geometry as shown in *Fig 7*. The amplitude is significantly enhanced in the animation to make the vibration visible. A cursor may be used to measure the position of nodes and anti-nodes at high precision.

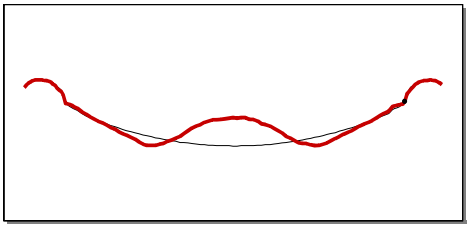

Enhanced displacement overlaid with cone profile

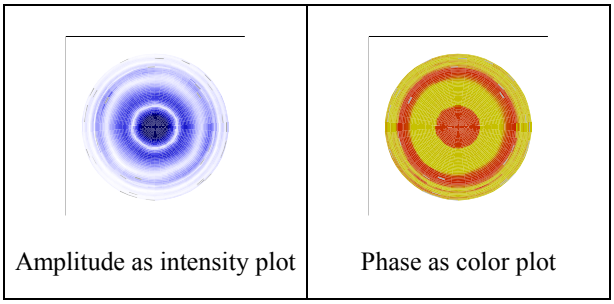

Amplitude as intensity plot	Phase as color plot

Fig 6: Styles for animation versus 2D geometry

Intensity + Phase	Phase only

Fig 7: Styles for 3D animation versus 3D geometry

For a sinusoidal stimulus a slow motion of the vibration can be animated by adding a rotating phase difference to the phase response of all points.

Although 2D and 3D animations are pretty images their practical value for loudspeaker design and diagnostics is limited for the following reason:

First, the phase coding reveals sources of positive and negative volume velocity on the surface of the radiator. However, not only the phase of the mechanical vibration but also the phase generated by sound propagation over the distance $|r_c\text{-}r_a|$ between the position r_c of the source and the receiving point r_a in the sound field decides whether a particular source makes a destructive or constructive contribution to the sound pressure at r_a.

Second, the animated displacement is interpreted as a relative quantity which is always bounded to a particular frequency and may be enhanced by the user to produce a display which satisfies optical and aesthetic requirements. All the 2D and 3D animations of the transfer function $H_x(j\omega,\vec{r_c})$ fail in quantitative assessment of the vibration and its impact on sound pressure output.

5. DERIVED MECHANICAL AND ACOUSTICAL CHARACTERISTICS

However, the basic vibration parameters and geometry contain valuable information which can be made available for loudspeaker design and diagnostics by deriving secondary parameters.

5.1. Sound Pressure Level

Using the Rayleigh integral the sound pressure

$$p(j\omega,\vec{r_a}) = \frac{\omega^2\rho_0}{2\pi}\int_{S_c}\frac{X(j\omega,\vec{r_c})}{\left|\vec{r_a}-\vec{r_c}\right|}e^{-jk\left|\vec{r_a}-\vec{r_c}\right|}dS_c \qquad (6)$$

and the related sound pressure level

$$SPL(\omega,\vec{r_a}) = 20\log\left(\frac{\left|p\left(j\omega,\vec{r_a}\right)\right|}{p_o}\right)dB \qquad (7)$$

at the point r_a in the sound field is calculated by integrating the acceleration at each point r_c weighted by each surface element dS_c, the distance between point r_a and the point r_c and using the density ρ_0 of air.

Although the Rayleigh integral provides only a useful approximation for relatively flat geometries operated in an infinite baffle, the low computational load of *Eq. (6)* makes it perfect for diagnostic purposes.

5.2. Accumulated Acceleration

Besides the acoustical output we need a quantity which describes the total mechanical energy in the radiator. Missing some geometrical information (e.g. thickness of the shell) and the material parameters (Young's E modulus) we can not calculate the kinetic and potential energy of the mechanical vibration based on scanning results.

However, it is possible to define an accumulated acceleration

$$a_a(j\omega,\vec{r}_a) = \frac{\omega^2\rho_0}{2\pi}\int_{S_c}\frac{\left|X(j\omega,\vec{r_c})\right|}{\left|r_a-r_c\right|}dS_c \qquad (8)$$

and the Accumulated Acceleration Level

$$AAL(\omega,\vec{r}_a) = 20\log\left(\frac{a_q(j\omega,\vec{r}_a)}{p_o}\right)\quad dB \qquad (9)$$

in dB which is almost identical with the Rayleigh integral but neglects the phase information both from the displacement and the sound propagation from point r_c to point r_a.

Thus, the AAL is a measure which summarizes the total vibration of the radiator in a energetic way but uses a weighting which makes the AAL comparable with the sound pressure output SPL. Both levels AAL and SPL are identical as long as all elements move in-phase (e.g. piston mode).

5.3. Decomposition in Radial and Circular Components

If the loudspeaker cone has a round shape and the measured displacement $X(r,\varphi)$ is expressed in polar coordinates depending on radius r and angle φ the total excursion

$$x_n(r,\varphi) = x_{cir}(r,\varphi) + \overline{x_{rad}}(r) \qquad (10)$$

can be split into a radial component $\overline{x_{rad}}(r,\varphi)$ and a circular component $x_{cir}(r,\varphi)$.

5.3.1. Radial Displacement Component

The radial component

$$\overline{x_{rad}}(r) = \frac{1}{2\pi}\sum_{\varphi=0}^{2\pi} x_n(r,\varphi) \qquad (11)$$

is calculated by averaging the displacement versus the angle φ. The radial component is useful for comparing the results of axial-symmetrical FEA with real measurements.

5.3.2. Circular Displacement Component

The circular component

$$x_{cir}(r,\varphi) = X(r,\varphi) - \overline{x_{rad}}(r) \qquad (12)$$

is the difference between total vibration and the radial component. The circular component reveals rocking modes and other circumferential modes.

5.4. Sound Pressure related Decomposition

The total vibration

$$X(\vec{r_c}) = x_{in}(\vec{r_c}) + x_{anti}(\vec{r_c}) + x_{quad}(\vec{r_c}) \qquad (13)$$

can be split into three components with different contribution to the sound pressure output (constructive, destructive, no effect).

5.4.1. In-Phase Component

The in-phase component

$$x_{in}(\vec{r_c}) = \mathrm{Re}_+\left\{X(\vec{r_c})\exp(j\arg(p(j\omega)) + jk(\vec{r_a} - \vec{r_c})\right\} \qquad (14)$$

contributes actively to the sound pressure output. The acceleration level AAL is identical with the sound pressure level SPL considering the in-phase component only.

5.4.2. Anti-Phase Component

The anti-phase component

$$x_{anti}(\vec{r_c}) = \mathrm{Re}_-\left\{X(\vec{r_c})\exp(j\arg(p(j\omega)) + jk(\vec{r_a} - \vec{r_c})\right\} \qquad (15)$$

contributes destructively to the sound pressure output. The SPL generated by the anti-phase component alone is identical with acceleration level AAL. The SPL and AAL of the anti-phase component is never higher than the SPL and AAL generated by the in-phase component.

5.4.3. Quadrature Component

The quadrature component

$$x_{quad}(\vec{r_c}) = \mathrm{Im}\left\{X(\vec{r_c})\exp(j\arg(p(j\omega)) + jk(\vec{r_a} - \vec{r_c})\right\} \qquad (16)$$

does not contribute to the sound pressure level SPL at point r_a because the total volume velocity of this component is always zero while the accumulated acceleration level (AAL) of the quadrature component is usually not negligible.

5.5. Mechanical Admittance

At the voice coil the distributed model of the radiator is linked with the lumped parameter model of the motor. The mechanical admittance

$$Y_{mech}(j\omega) = \frac{V_{coil}(j\omega)}{F_{coil}(j\omega)} \qquad (17)$$

is the ratio of the complex velocity V_{coil} and the driving force F_{coil} of the coil. For axial-symmetrical voice coil formers the velocity V_{coil} can calculated by using the differentiated radial displacement $\overline{x_{rad}}(r_{coil})$ averaged over angle φ at radius r_{coil} and the force F_{coil} can be estimated by using the dc resistance R_e, the inductance L_e of the voice coil and the moving mass M_{ms} yielding the admittance

$$Y_{mech}(j\omega) = \frac{j\omega\overline{x_{rad}}(j\omega, r_{coil})}{F_{coil}(j\omega)} \approx \frac{j\omega H_x(j\omega, r_{coil})(R_e + j\omega L_e)}{Bl + H_x(j\omega, r_{coil})\omega^2 M_{ms}(R_e + j\omega L_e)} \quad (18)$$

If the moving mass M_{ms} is negligible compared to the mechanical admittance at higher frequencies and $|Y_{mech}(j\omega)M_{ms}j\omega| < 1$ the admittance can be approximated by

$$Y_{mech}(j\omega) \approx \frac{j\omega H_x(j\omega, r_{coil})(R_e + j\omega L_e)}{Bl}. \quad (19)$$

Thus the amplitude response of the displacement transfer function $H_x(j\omega,r_{coil})$ reveals dips and peaks which indicate the resonance and anti-resonance frequencies of the panel.

5.6. Modal Analysis

The vibration of a mechanical structure can also be investigated in the modal space where the total vibration can be expanded into a series

$$X(j\omega, \vec{r_c}) = \sum_{i=0}^{\infty} \frac{\psi_i(\vec{r_c})}{1 + \eta_i j\omega/\omega_i - (\omega/\omega_i)^2} \quad (20)$$

of independent vibration modes characterized by a natural function $\psi_i(\vec{r_c})$ and a frequency dependent term in the denominator. The function $\psi_i(\vec{r_c})$ describes the mode shape of the vibration mode i on the radiator's surface and is independent of frequency. The denominator comprises two poles which generate a 2nd order resonance at the natural frequency ω_i. The sharpness of the resonance peak at ω_i is determined by the loss factor η_i.

The accumulated acceleration

$$a_a(j\omega) = \frac{\rho_0}{2\pi} \sum_{i=0}^{\infty} \frac{\omega^2}{1 + \eta_i j\omega/\omega_i - (\omega/\omega_i)^2} \int_{S_c} \frac{|\psi_i(\vec{r_c})|}{|r_a - r_c|} dS_c \quad (21)$$

can be also developed as a sum of modes where each element contains a frequency depending term (high-pass) and an integral which summarizes the amplitude of the natural function $\psi_i(\vec{r_c})$ on the radiator. The distance $|r_a\text{-}r_c|$ is almost constant if r_a is in the far field. The important point is that the poles in the high-pass term in *Eq. (21)* are identical with the poles in low-pass term in *Eq. (20)*.

5.6.1. Natural Frequency

The loss factor η_i is relatively small (η_i < 0.1) in materials used for radiators and the modal resonances generate distinct peaks in the amplitude response of a_a. Thus the natural frequencies can be easily found by searching for frequencies in the amplitude response where AAL produces a local maxima.

5.6.2. Natural Function

On most structures used as radiators in loudspeakers the modal density is relatively low (DML is an assumption) and the loss factor is usually small. The amplitude of the i^{th}-mode decreases rapidly with the distance from the natural frequency and the contribution to the total sound pressure at the adjacent natural frequency of the next mode. Therefore, the i^{th}-order natural function

$$\psi_i(\vec{r_c}) \approx X(j\omega_i, \vec{r_c}) \quad (22)$$

can be approximated by the total displacement at the natural frequency ω_i.

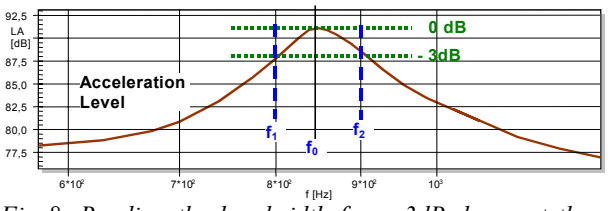

Fig 8: Reading the bandwidth for a 3dB decay at the natural frequency in the accumulated acceleration level.

5.6.3. The loss factor

The modal loss factor can be defined by the relative bandwidth

$$\eta_i = \frac{\omega_{i+} - \omega_{i-}}{\omega_i} \qquad (23)$$

using the natural frequency ω_i, the lower frequency ω_{i-} and the upper frequency ω_{i+}. As illustrated in *Fig 8* the lower frequency $(\omega_{i-}<\omega_i)$ is found at the 3dB decay of the acceleration level $AAL(\omega_{i-}) = AAL(\omega_i) - 3dB$ and upper frequency $(\omega_{i+}<\omega_i)$ is found at $AAL(\omega_{i+}) = AAL(\omega_i) - 3dB$.

6. DIAGNOSTICS OF VIBRATION AND RADIATION PROBLEMS

The vibration and geometry parameters of the drive unit are already a good basis for analyzing the physical causes of dominant problems in the radiated sound. This shall be illustrated on following drive units:

- Woofer A using a conventional 11 cm paper cone
- Woofer B using a 11 cm inch magnesium cone
- Woofer C using a 12 cm flat piston as radiator
- Horn compression driver with a 6 cm aluminum dome.

The drive units are operated virtually in an infinite baffle and the radiation into the half space is investigated. The influence of the enclosure, horn and acoustical system which is finally coupled to the drive unit is neglected. For this kind of diagnostics the Rayleigh equation is a sufficient approximation at minimal computational load.

6.1. Smooth SPL Response ?

Significant peak and dips in the sound pressure response impair the sound quality and are perceived as coloration. In the first step of the analysis the SPL response is calculated at a point on axis and a few degrees out of axis. Those responses may represent the direct sound varying over the listening area. The flatness and smoothness of the responses are investigated and the critical frequencies are determined.

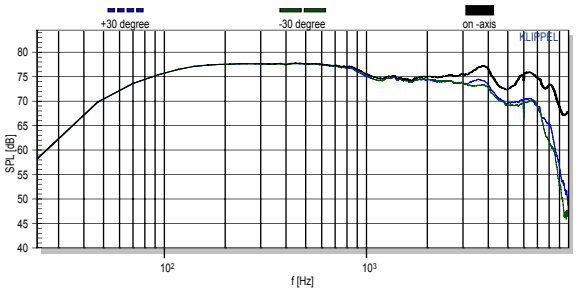

Fig 9: Predicted sound pressure response on-axis and two points +/- 30^0 out of axis of woofer A with a paper cone.

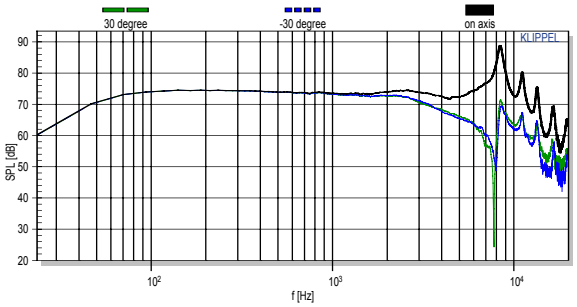

Fig 10: Predicted sound pressure response on-axis and two points +/- 30^0 out of axis of woofer B with a magnesium cone.

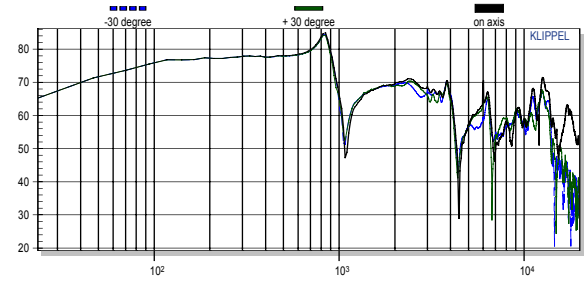

Fig 11: Predicted sound pressure response on-axis and two points +/- 300 out of axis of woofer C with a flat radiator.

Fig 9 shows a relatively flat and smooth SPL response of woofer A using a conventional paper cone. At 1 kHz the SPL on-axis and +- 30 degree off-axis drops by 3 dB but then it stays constant up to 4 kHz. *Fig 10* shows the on-axis SPL response as thick solid line of woofer B using a magnesium cone which is almost constant up to 6 kHz. Only the SPL response measured +/- 30 degree out of axis decreases above 2 kHz. The distinct peaks above 8 kHz are not relevant for a woofer application. *Fig 11* shows the SPL responses of woofer C using a flat piston as radiator. There is a 6dB peak at 800 Hz and a significant dip at 1.1kHz both in on-axis and off-

axis responses which is not acceptable for the particular application.

6.2. Desired Directivity ?

For critical frequencies (where the peaks and dips occur) it is useful to investigate the variation of the SPL over a larger number of the angles. This is important for the radiated sound power response which determines the diffuse sound in enclosed spaces (rooms).

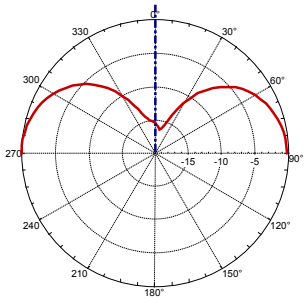

Fig 12: Directivity of SPL in the horizontal plane predicted for woofer C at 1.1 kHz.

Fig 12 shows for example the directivity of woofer C at the critical frequency 1.1 kHz which indicates that the dip is limited to a narrow angle and the sound power response is less affected than the on-axis response.

6.3. Sufficient Cone Vibration?

Without cone vibration there is no radiated sound! The analysis of the cone vibration should start with the calculation of the accumulated acceleration level (AAL). This level shows the maximal possible SPL by summarizing the volume velocity of all points on the radiator's surface while neglecting phase differences.

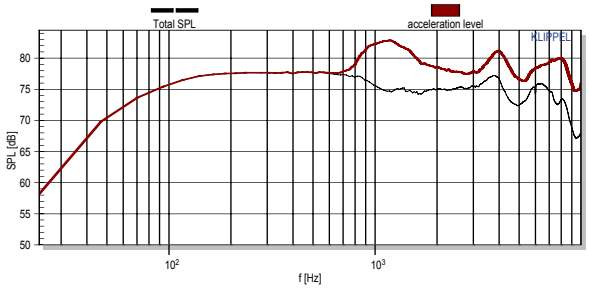

Fig 13: Response of the accumulated acceleration level (thick line) compared to the total sound pressure level (thin line) of woofer A with a paper cone

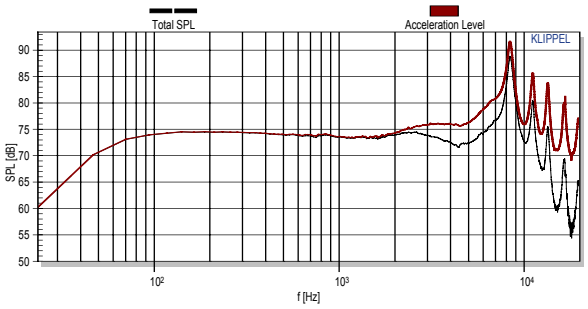

Fig 14: Response of the accumulated acceleration level (thick line) compared to the total sound pressure level (thin line) of woofer B with a magnesium cone.

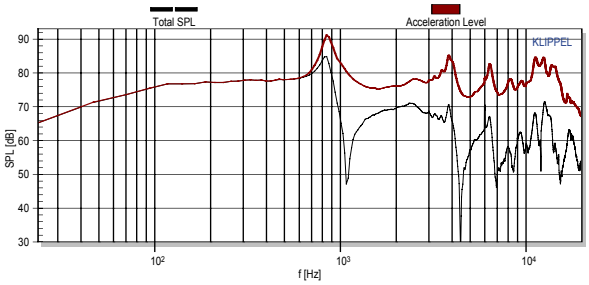

Fig 15: Response of the accumulated acceleration level (thick line) compared to the total sound pressure level (thin line) of woofer C with a flat radiator

The acceleration level is identical with the on-axis SPL response at lower frequencies where the cone vibrates as a rigid body and no acoustical cancellation occurs. At higher frequencies there are peaks in the acceleration level which are placed at the natural frequencies of the mechanical modes.

The woofer A with the paper cone produces a peak in AAL at 1.1 kHz as shown in *Fig 13* which is not visible in the SPL response. The dip in the SPL response at 5 kHz corresponds with a lack of accumulated acceleration. For woofer B with the magnesium cone both AAL and SPL responses are identical up to 2 kHz as shown in *Fig 14*. The acceleration stays also constant up to 4 kHz and shows significant peaks of 10 –15 dB at the natural frequencies. Above 10 kHz where the moving mass of the coil dominates the total mechanical impedance the AAL decreases dramatically.

Fig 15 shows that the acceleration level of woofer C with the flat piston has a peak of 10 dB at 850 Hz which causes the first peak in the SPL response while the other peaks at 4 kHz and higher do not generate excessive peaks in SPL. It is interesting to see that there are no sharp dips in the acceleration level. Above 15 kHz the acceleration level also decreases due to the influence of the coil mass.

6.4. What indicates cone break-up ?

The ring anti-resonance is the precursor of the first bending mode. At this frequency f_{ra} the mass and the longitudinal stiffness of the outer ring zone build up a resonating system.

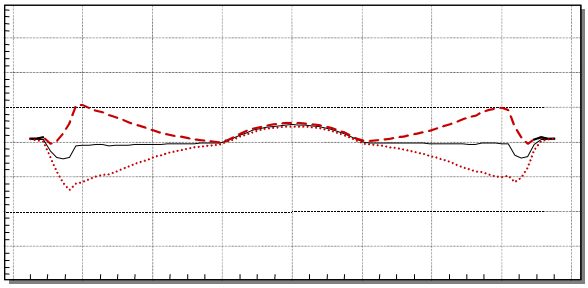

Fig 16: Sectional view of the woofer C (thin line) and positive and negative peak displacement (dashed and dotted line, respectively) at the ring anti-resonance frequency f_{ra}.

A high transverse displacement of the outer ring zone occurs at the ring anti-resonance frequency f_{ra} = 632 Hz as shown in *Fig 16*. This causes a bending moment in the shell which leads to a bending mode at higher frequencies.

At the ring anti-resonance frequency f_{ra} the high displacement at the ring zone corresponds with a low displacement at the voice coil where the cone is excited. Thus it is called an "anti"-resonance. This frequency can be found by searching for a local minimum in the amplitude response as discussed in *Fig 4* which corresponds with a minimum of the mechanical admittance as shown in *Eq. (18)*.

The anti-resonance frequency f_{ra} does not produce a significant peak neither in the AAL response nor in the SPL response in *Fig 15*.

6.5. What causes peaks in SPL response ?

All peaks in the SPL response already appear in the acceleration response AAL. The peaks corresponds with the natural frequencies ω_i of the vibration modes $\psi_i(\vec{r}_c)$ on the cone and cause the poles in the rational transfer function in *Eq. (20)*.

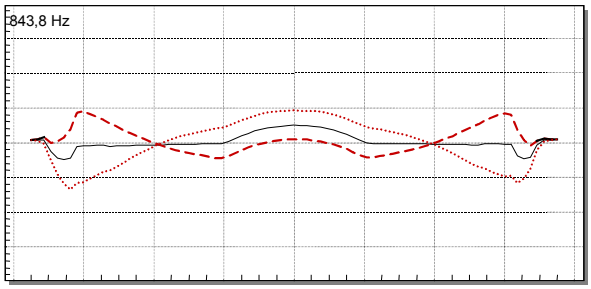

Fig 17: Sectional view of woofer C (thin line) and positive and negative peak displacement (dashed and dotted line, respectively) at the first bending resonance frequency f_{b1}.

The flat piston used as radiator in woofer A shows the first bending mode at f_{b1}=843 Hz as shown in *Fig. 17*. At this frequency the amplitude of the displacement in *Fig 4* and the acceleration AAL in *Fig 15* becomes maximal.

6.6. Sufficient Damping of the Material ?

Losses in the cone material are required to keep the *Q* factor of each cone resonance sufficiently low. This is important to avoid significant peaks in the SPL response and transient distortion in the cumulative decay spectrum which are related with rapid variations of the phase response versus frequency.

The modal loss factor which is the inverse of the Q factor can be calculated by using *Eq. (23)* and the 3dB bandwidth.

The loss factor η_i of the composite material used as a flat radiator is about 0.1 at first natural frequency 850 Hz. To suppress the peak in the SPL response the loss factor has to be increased by factor 2 or more. The damping can be increased by replacing the material of the radiator or by applying a partial coating of the surface with a viscous material. A coating of the complete radiator surface is usually not required for damping particular modes but the additional moving mass will reduce the sensitivity.

6.7. Where to apply additional damping ?

The coating should be applied to the region where the natural mode generates a high value of longitudinal velocity in meridional direction (from coil to surround). Since the first bending mode of the 5 inch example driver covers almost the whole flat disc part everything should be coated by a damping material except the dome at the centre of the radiator.

Alternatively, also the loss factor of the surround material could be increased.

6.8. What causes dips in SPL response ?

The difference between the SPL output and the accumulated acceleration AAL level is caused by a partial compensation of the volume velocities generated by the points on the radiators surface. A complete acoustical cancellation generates a zero in the transfer function in *Eq. (1)*. In this case the in-phase component and the anti-phase component have the same acceleration level AAL which is identical with the SPL generated by each component.

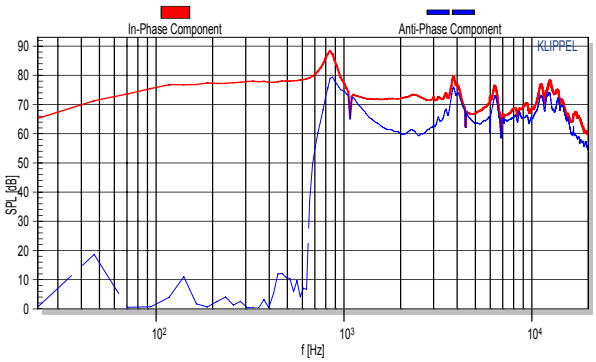

Fig 18: AAL and SPL Response of the in-phase component and anti-phase component of woofer C with flat radiator.

Fig. 18 shows the accumulated acceleration level AAL for the 5 inch example drive unit. In the piston mode the anti-phase component is almost negligible and would only produce 20 dB output if the other components are not considered. Above the ring anti-resonance frequency f_{ra}=632 Hz the anti-phase component rises steadily and becomes maximal at the first bending mode f_{b1}=843 Hz. At this frequency the anti-phase component is almost 10dB below the in-phase component. The acoustical cancellation occurs at 1.1kHz, 4.4kHz and 7kHz where the in-phase and anti-phase components become identical.

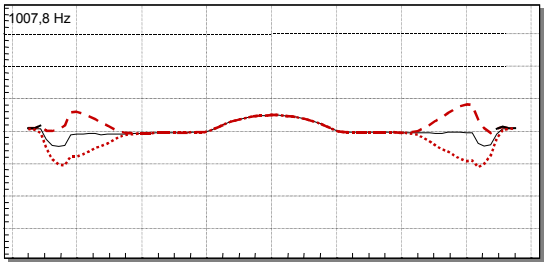

Fig 19: Sectional view of woofer C with (thin line) and positive and negative peak displacement (dashed and dotted line, respectively) of the in-phase component at 1007 Hz.

The location of the in-phase component gives a deeper understanding of the cancellation process at 1.1kHz. Passing the cancellation frequency the in-phase component moves from the outside ring to the centre of the piston as shown in *Fig. 19* and *20*.

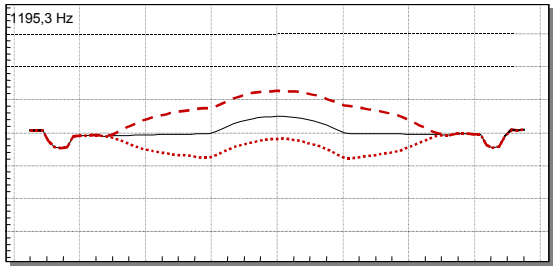

Fig 20: Sectional view of the 5 woofer C (thin line) and positive and negative peak displacement (dashed and dotted line, respectively) of the in-phase component at 1195 Hz.

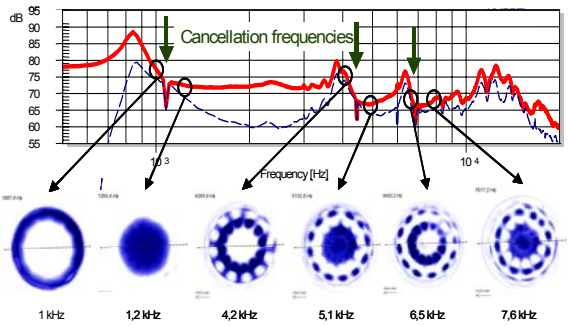

Fig 21: SPL response (thick solid line) and intensity plot of the in-phase component compared with the SPL response (dashed line) of the anti-phase component of woofer C with a flat radiator.

The in-phase component switches its position also at 4.4 kHz, 7 kHz, 8.5 kHz, 10 kHz and 15 kHz just at the frequencies where the SPL (or AAL) of the in-phase component equals the anti-phase component.

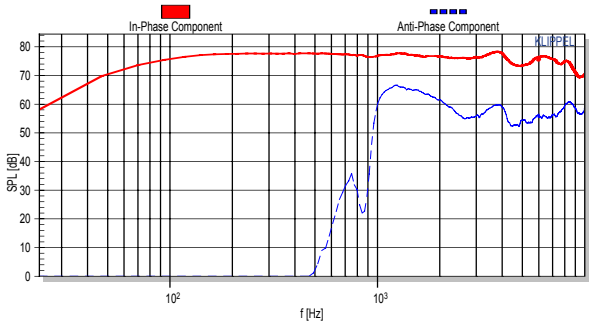

Fig 22: SPL response of the in-phase component (thick solid line) compared with the SPL response of the anti-phase component (dashed line) of woofer A using a paper cone.

Loudspeaker with a dominant in-phase component which is at least 6 dB higher in SPL (or AAL) than the anti-phase component will not suffer from acoustical cancellation.

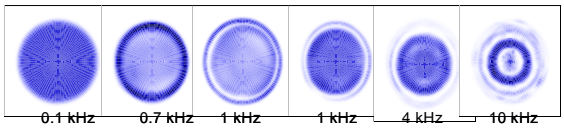

Fig 23: Intensity plot of the in-phase component at various frequencies of woofer A using a paper cone.

Woofer A and B using a conventional paper and magnesium cone, respectively, show a completely different behavior. The SPL (AAL) of the anti-phase component in *Fig. 22* and *24* is always more than 10 dB below the in-phase component. Therefore, there are no acoustical cancellation effects causing dips in the SPL response. The anti-phase components generated above the ring anti-resonance frequency f_{ra} spread with rising frequency from the outside edge to the center and push the in-phase back to the inner region of the cone as shown in *Fig. 23* and *25*. Like that both cones reduce their effective radiation area towards higher frequencies. This also reduces the effective moving mass as seen by the driving force generated by the coil which increases the real part of the acoustical radiation impedance and likewise the acoustical output power. Furthermore the radiation at higher frequencies becomes less directive because of the shrinking size of the effective radiation area. Both effects make it possible to build drive units which can be used over the full audio band.

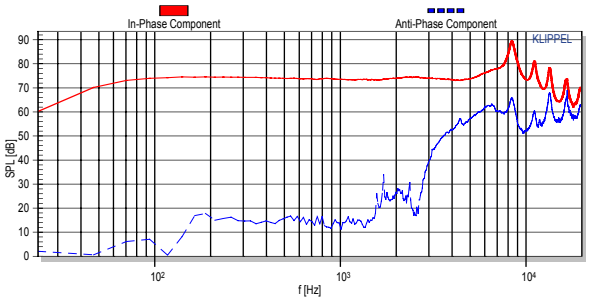

Fig 24: SPL response of the in-phase component (thick solid line) compared with the SPL response of the anti-phase component (dashed line) of woofer B using a magnesium cone.

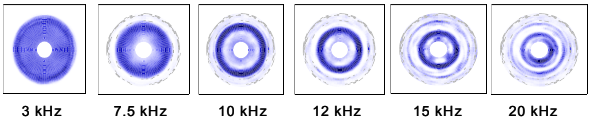

Fig 25: Intensity plot of the in-phase component at various frequencies of woofer B using a magnesium cone.

6.9. How to avoid acoustical cancellation ?

The SPL or AAL of the in-phase component should be at least 6 dB higher than the SPL or AAL of the anti-phase component to avoid acoustical cancellation and dips in the total SPL response. If the in-phase component is always dominant it will be bounded to a fixed region on the radiator's surface which shrinks in size at higher frequencies. Conventional cones with an apex angle less than 70 degree break up gradually from outside. The first node occurs close to the outer rim because the shell is there less curved than towards the center and the bending stiffness is much lower.

Piston drivers such as used in woofer C or flat cones with a high apex angle (> 70 degree) generate a first node which is located closer to the centre leading to a strong anti-phase component. Using a material with a different Young's *E* modulus will usually not solve this problem because the cancellation point will only be shifted in frequency but the mode shape remains very similar. A variation of the loss factor will not solve the cancellation problem either. The only solution is to change the shape of the mode by varying the distributed mass or bending stiffness on the shell versus radius *r*. This can be accomplished by using a shell which becomes thicker for lower radii or placing additional rips below the radiator in the inner region which increases the bending stiffness there while keeping a low bending stiffness in the outside region. Thus, also a flat radiator will have its first bending node closer to the

outer rim and gets a dominant in-phase component in the center of the radiator as illustrated in *Fig. 26*.

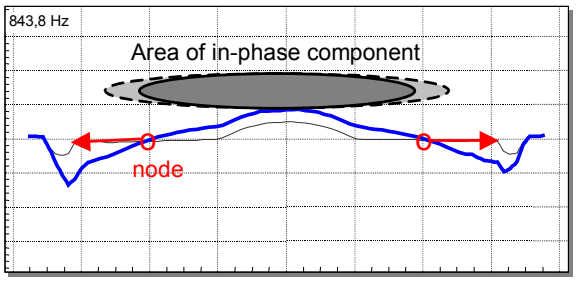

Fig 26: Increasing the piston area of the in-phase component by increasing the bending stiffness in the center of the cone.

6.10. Dominant circumferential modes ?

Loudspeaker drive units with a round shape do not only show modes in radial direction but also in circular direction. Circular modes may become more dominant in case there are any irregularities at the circumference such as wires or e.g. additional 12 rips below the radiator in woofer C as shown in *Fig. 27*.

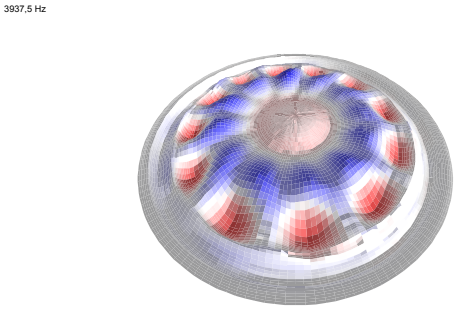

Fig 27: Geometry of the flat piston used in woofer C and animated total displacement at 4 kHz.

Since woofer C has an axial-symmetrical shape the decomposition technique of *Eq. (10)* can be applied. The acceleration level of the circular component shown as thick solid line in Fig. 28 is at higher natural frequencies only 3 dB below the total acceleration level shown as dashed line.

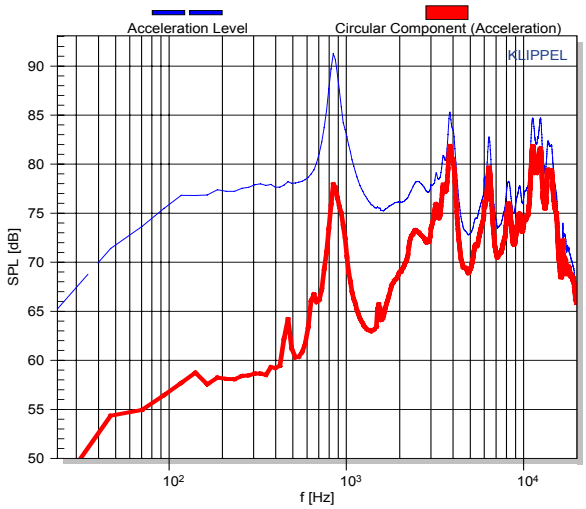

Fig 28: Accumulated acceleration level of the circular component (thick curve) and the total vibration (dashed curve) of Woofer C.

Although the circular component has high mechanical energy it generates 50 dB less SPL on-axis rectangular to the radiator's plane as shown as thick solid curve in *Fig. 29*. The radial component generates the dominant contribution to the on-axis SPL (thin curve) which is 40 db higher than the SPL output of the circular mode.

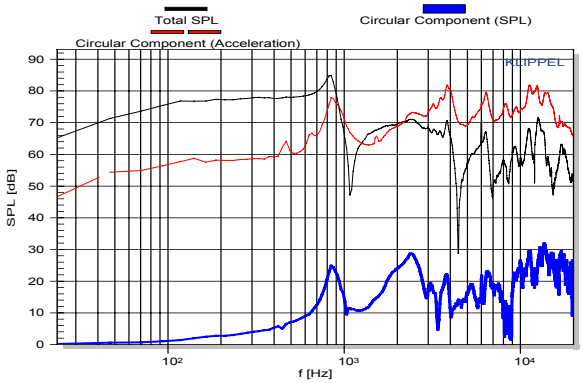

Fig 29: Accumulated acceleration level AAL (dashed curve) and sound pressure level SPL (thick curve) of the circular component compared with the SPL of the total component (thin curve) of woofer C on axis.

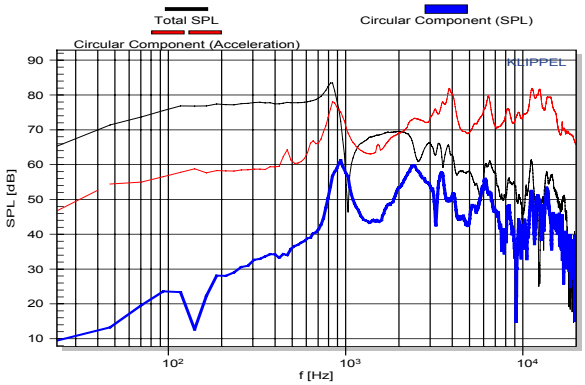

Fig 30: Accumulated acceleration level AAL (dashed curve) and sound pressure level SPL (thick curve) of the circular component compared with the total SPL (thin curve) at 60 degree out of axis.

For a measurement point which is 60 degree out of axis the SPL of the circular component shown in Fig. 30 as thick solid curve is 30 dB higher and contributes to the total SPL output significantly.

The directivity plots of the circular component reveal in *Fig. 31* a high SPL output for high angles off axis at all frequencies. Thus circular components which do not have much impact on the on-axis response may be important for reducing the directivity of a speaker producing a dispersive sound.

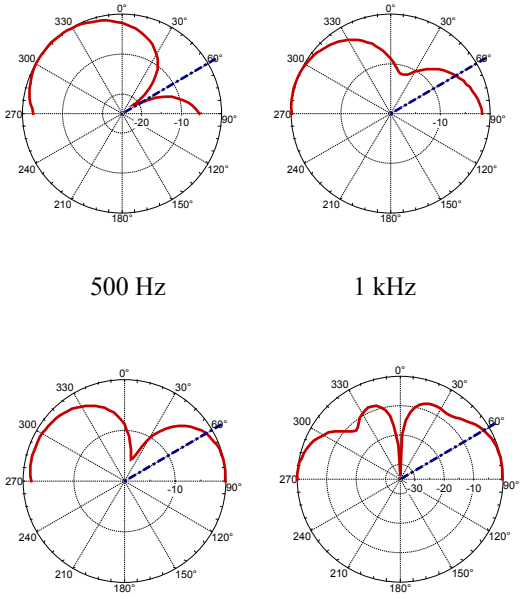

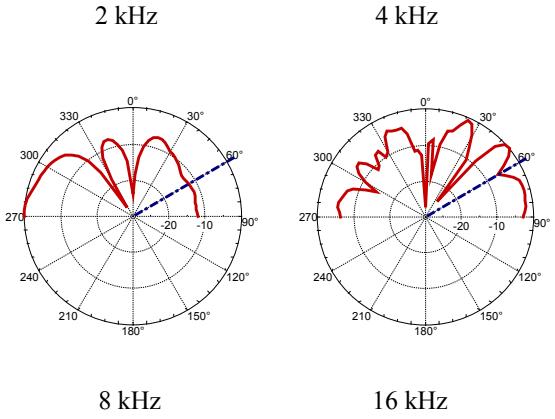

Fig 31: SPL directivity measured at 1 m in the horizontal plane generated by the circular vibration component of woofer C at various frequencies.

6.11. Rocking modes ?

The first circumferential mode on the surround causes a rocking movement of the cone and a tilting of the voice coil former. This may cause a rubbing of the voice coil in the gap which could produce audible distortion and could even lead to a permanent damage of the speaker. Rocking modes do not contribute significantly to the total sound pressure output. The best indicator for rocking modes and any other circumferential modes is the accumulated acceleration level (AAL) of the quadrature component.

Below cone break-up where the acceleration level of the quadrature component is much smaller than the total component there is a distinct peak at 380 Hz in *Fig 32*. This is caused by a rocking mode of woofer A as shown in *Fig 33*.

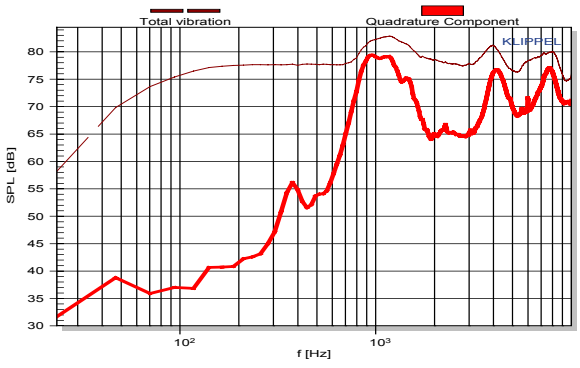

Fig 32: Accumulated acceleration level (AAL) of the quadrature component (solid curve) compared with the

total component (dashed curve) of woofer A using a paper cone.

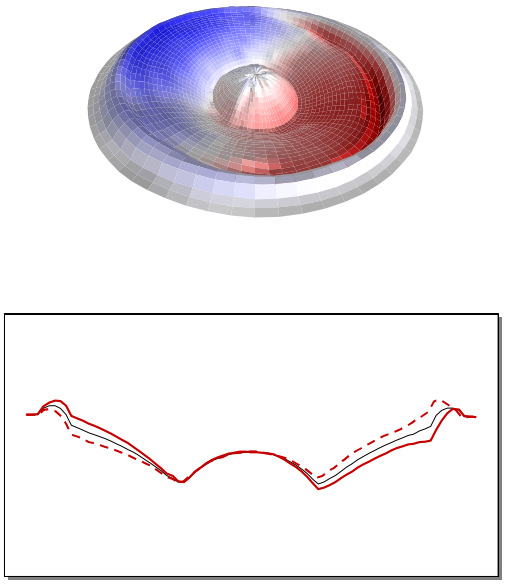

Fig 33: Vibration of the paper cone of Woofer A at 400 Hz .

Clearly the paper cone itself behaves like a rigid shell but the rocking mode causes significant deformation of the surround. Flat loudspeakers using a low cone height and headphones and micro-speakers dispensing with a spider are prone to rocking modes. Any angular variation of the stiffness of the surround and the additional inertia of the wires initialize and support rocking modes. Rocking modes may have significant amplitude in the acceleration level but can hardly be detected in the radiated sound pressure output.

6.12. Irregular Vibrations ?

Irregular vibrations are not expected and can usually not be predicted by finite element analysis. The contribution of most irregularities to the total sound pressure is relatively small but the irregular vibration may cause excessive nonlinear distortion because the local displacement may be high. Peaks in the frequency response of the accumulated acceleration level of the quadrature component is a good indicator for such vibrations. For loudspeaker drive units with an axial-symmetrical shape the AAL response of the circular component is a powerful alternative.

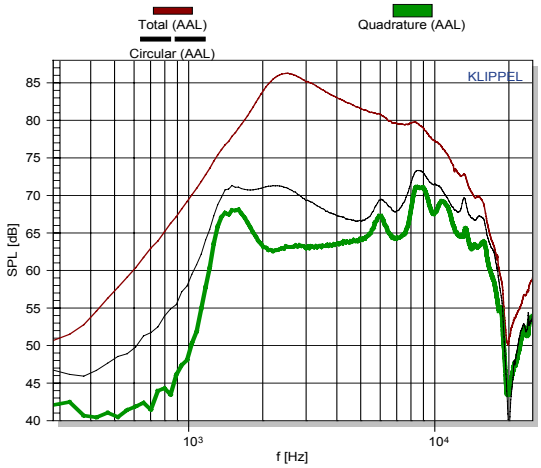

Fig 34: Accumulated acceleration level (AAL) of the quadrature component (thick solid curve), circular (dashed curve) and total component (thin solid curve) of a horn compression driver using an aluminum dome.

The scanning data of a horn compression driver reveals a small peak in the AAL response of both circular and quadrature components in *Fig 34* which is not visible in the total AAL and SPL response. *Fig 35* shows that a small region close to the center of the dome vibrates at much higher displacement at 6 kHz.

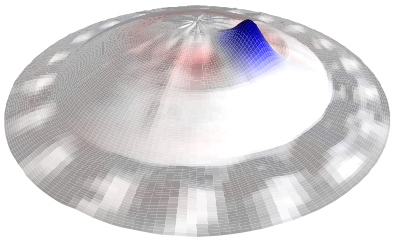

Fig 35: Irregular vibration pattern caused by varying thickness of an aluminum dome in a horn compression driver at 6 kHz.

Such irregularities may be caused by unbalanced mass distributions, non-uniform density or thickness of the shell and intended folds and corrugations.

6.13. Causes of Harmonic Distortion ?

The measurement of the nonlinear distortion in the mechanical signal puts high requirements on the signal-to-noise-ratio of the used sensor. A conventional measurement of the harmonic distortion in the sound pressure output can be realized more easily by using a microphone. A filtering of the measured distortion signal by the inverse fundamental response gives the

equivalent input distortion which is presented for woofer B in *Fig. 36*.

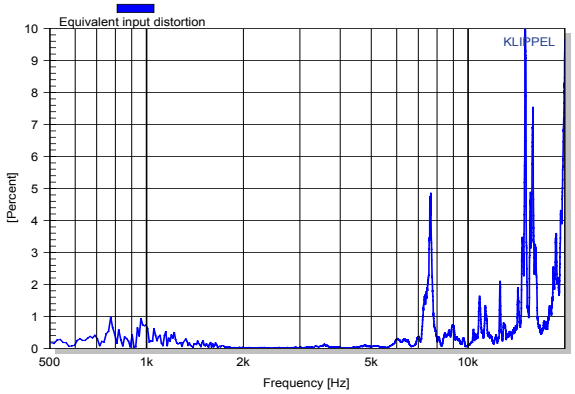

Fig 36: Equivalent input distortion measured in the sound pressure output of woofer B with the magnesium cone.

For low and medium frequencies where the magnesium cone vibrates as a rigid body the distortion is below 1% but at the natural frequencies of the bending modes there can be seen significant peaks which correspond with peaks in the acceleration level in *Fig. 14*. Applying a coating of additional damping material to the magnesium dome would not only make the SPL response smoother but would also reduce the distortion generated at those frequencies.

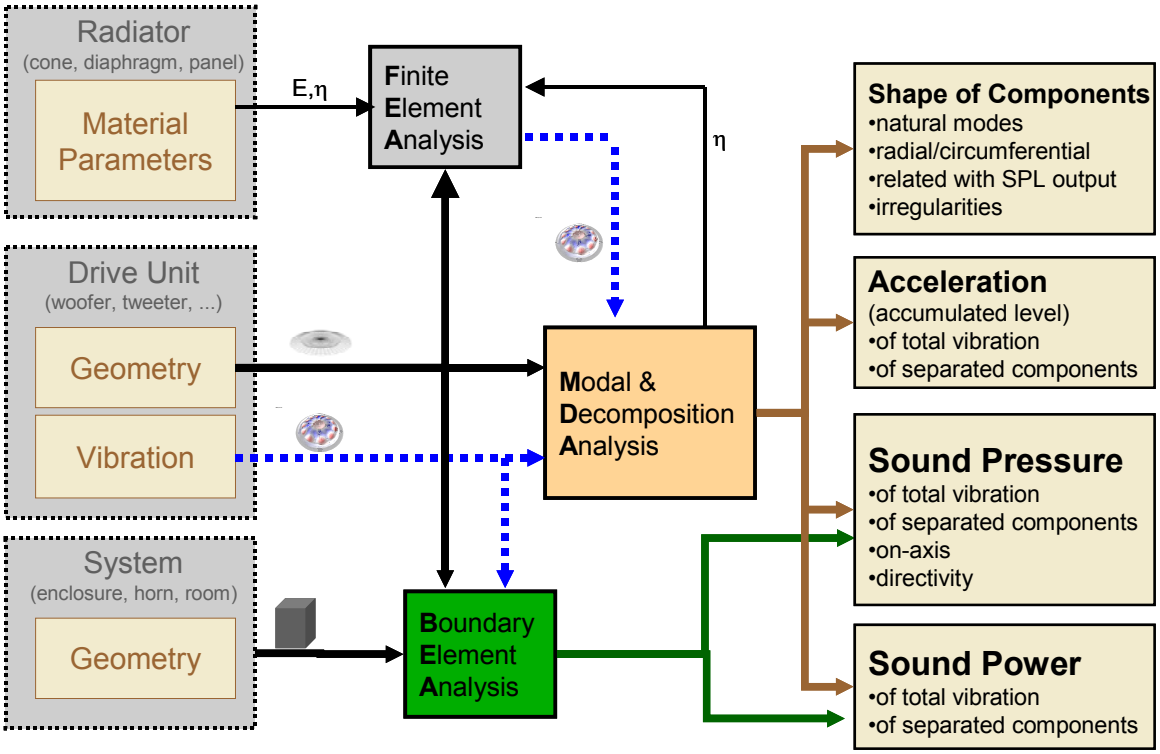

Fig 37: Overview on vibration and radiation analysis in loudspeaker design

7. CONSEQUENCES FOR LOUDSPEAKER DESIGN

The measurement of the mechanical vibration of the drive unit is the basis for vibration and radiation analysis which makes the relationship between geometry and material properties of the radiator and the sound pressure output more transparent. The previous part of the paper discussed the measurement of a drive unit and showed that basic diagnostics can be accomplished by using only scanning data (surface geometry and transfer functions) as illustrated in *Fig 37*. The simple monopole approximation in *Eq. (6)* and the

related equation of the accumulated acceleration level in *Eq. (8)* enable modal and decomposition analyses to show the effect of separated components and modes. The following paragraph describes how these diagnostics can imbedded in the design process and linked to simulation tools (FEA and BEA) requiring additional parameters as input.

7.1. Cone & Drive Unit

The basic diagnostics usually provide some ideas for improvements and indicate (re-)design choices which have to be verified. Instead of building new prototypes it is more time effective to use finite element analysis for the verification as illustrated in *Fig 37*.

The most basic input parameters for an finite element analysis (FEA) is the geometry, Young's $E(f)$ modulus and the loss factor $\eta(f)$ versus frequency f of the radiator (e.g. cone, surround) itself, but also of motor and suspension parts (e.g. voice coil former, spider). The geometrical parameters provided by the scanning process describe the external surface of the radiator at high precision. However, the thickness of the vibrating shell has to be measured separately and has a high impact on the natural frequencies of the bending modes. The loss factor $\eta(f)$ can be approximated by the modal loss factor $\eta(f_i)$ determined by the 3dB decay at the natural frequencies f_i in the accumulated acceleration response. The Young's modulus $E(f)$ highly depends on frequency and temperature and precise data is usually not available. The frequency dependency of $E(f)$ can be found by fitting the accumulated acceleration response (total AAL) as predicted by FEA to the response measured by scanning. The fitting of the AAL responses is much simpler than the fitting of SPL response at one measurement point which have a much more complex shape and are affected by the acoustical radiation conditions (geometry of the enclosure or baffle).

A full 3D FEA software is required to describe drive units with a non-circular shape and to consider circumferential modes on round radiators. However, a 3D FEA produces high computational load and requires input parameters such as non-uniform mass distribution which can not easily be provided. Thus, 2D FEA assuming axial symmetry is in many cases more practical. The results of axial-symmetrical FEA shall be compared with the AAL of the radial component to suppress circumferential modes found in the measured vibration.

7.2. Loudspeaker System & Room

If the accumulated acceleration response predicted by FEA agrees with the AAL response derived from the scanned vibration, then the sound pressure output can be predicted at any point in the sound field by using boundary element analysis (BEA). This technique is based on the Kirchhoff equation and determines in the first step the sound pressure at the radiator itself and other acoustical boundaries (enclosure) as illustrated by the sound pressure distribution in *Fig 38* of woofer A mounted in a small enclosure. In the second step the sound pressure at any point in the far field can be calculated by simply calculating the surface integral using the calculated sound pressure and measured velocity on the boundary. This approach is more precise than the Rayleigh integral which considers only the volume velocity at the radiator's surface but is a surprisingly good approximation for the SPL on axis and for small angles out of axis especially if the radiator is flat and operated in an infinite baffle. The Rayleigh integral completely fails if there is no free sound propagation between the transmitting source at the radiator and the receiving point in the far field and also neglects diffraction, which is an important part of the sound propagation.

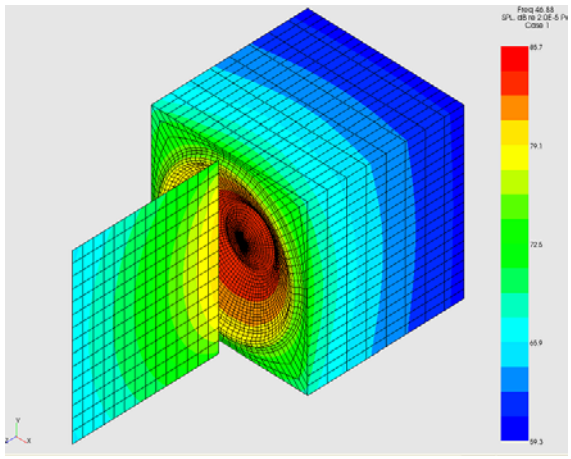

Fig 38: SPL at 1.1 kHz in the near field of woofer A mounted in a sealed enclosure predicted by boundary element analysis.

Thus, BEA should be used if the drive unit is mounted in an enclosure and a precise prediction of the SPL in small rooms (e.g. cars) is required.

BEA is very powerful for optimizing the geometry of the enclosure, horns, acoustical lenses and other means for guiding the sound and for considering the impact of boundaries in small rooms (e.g. cars). This design step can be done virtually by using the geometry of the

radiator and the measured vibration data as input parameters.

8. CONCLUSION

The properties of the loudspeaker drive unit which are relevant for the acoustical output can be described by a set of distributed parameters comprising the measured mechanical vibration and the geometry of the radiator's surface. The vibration is described by a complex transfer function between a reference signal (e.g. input voltage) and the motional signal (e.g. displacement) supplemented with the precise position of the measurement point in Cartesian or cylinder coordinates. A measurement grid comprising about 100 points provides sufficient accuracy for predicting the sound pressure output. Scans with higher resolution are required to detect local irregularities which affect only a small part of the radiator. The drive units may be scanned in free air or mounted in the final enclosure to consider the acoustical load of the sound field. Alternatively, the drive unit can also be measured in vacuum to consider the mechanical system only.

The measurement of the transfer functions is performed in the small signal domain to generate characteristics which are independent on the signal properties and supplement the linear, nonlinear and thermal parameters of the loudspeaker.

The distributed mechanical parameters open new ways for loudspeaker diagnostics. Modal analysis and novel decomposition techniques show the relationship between single components of the vibration and the impact on the sound pressure output. For this kind of analysis the Rayleigh equation is a useful approximation of the prediction of the SPL output and a basis for defining an accumulated acceleration level (AAL). Although the AAL describes the total mechanical energy on the radiator, this measure is directly comparable to the SPL predicted by the Rayleigh integral. This analysis gives indications for variations in the sound pressure response, generation of harmonic distortion and voice coil rubbing caused by rocking modes.

Those indications may be further investigated by FEA giving new ideas for design choices.

The distributed mechanical parameters calculated by a simulation or measured on a prototype may be also used for an accurate prediction of the sound pressure output by considering the acoustical environment (baffle, enclosure or horn) in a boundary element analysis to reach an optimal loudspeaker system design.

9. REFERENCES

[1] F.J.M. Frankort, "Vibration Patterns and Radiation Behavior of Loudspeaker Cones", *J. of Audio Eng. Soc.*, Vol. 26, Nr. 9, pp. 609-622 (September 1978).

[2] "Sound System Equipment – Electroacoustical Transducers – Measurement of Large Signal Parameters", IEC Publication PAS 62458 © IEC:2006(E).

[3] R. Small, "Closed-Box Loudspeaker System", *J. of Audio Eng. Soc*., Vol. 20, Nr. 10, pp. 798–808 (December 1972).

[4] W. Klippel, "Nonlinear Modeling of the Heat Transfer in Loudspeakers", *J. of Audio Eng. Soc.*, Vol. 52, No. 1/2, pp. 3-25 (February 2004).

[5] C. Struck, "Analysis of the Nonrigid Behavior of a Loudspeaker Diaphragm using Modal Analysis", *presented at 86th convention of Audio Eng. Soc*., Hamburg, preprint 2779 (1989).

[6] A. J. M. Kaizer, A. D. Leeuwestein, "Calculation of the Sound Radiation of a Nonrigid Loudspeaker Diaphragm Using the Finite-Element Method", *J. of Audio Eng. Soc*., Vol. 36, No. 7/8, pp. 539-551 (July 1988).

[7] D. A. Barlow, et. al., "The Resonances of Loudspeaker Diaphragms," *presented at the 65th Convention of the Audio Eng. Soc.*, preprint 1590 (February 1980).

[8] T. Heed, "Minimizing the Amplitudes of Transverse Modal Waves in Diaphragms," *presented at the 101st Convention of the Audio Eng. Soc.*, Los Angeles, preprint 4333 (November 1996).

[9] W. Klippel, J. Schlechter, "Measurement and Visualization of Loudspeaker Cone Vibration", *presented at the 121st Convention of the Audio Eng. Soc.*, New York, USA, preprint 6882, (October 2006).

[10] W. Klippel, "Measurement and Application of Equivalent Input Distortion," *J. of Audio Eng. Soc.*, Vol. 52, No. 9, pp. 931-947 (September 2004).